

In vivo behavior of calcium phosphate scaffolds with four different pore sizes

Marie-Cécile von Doernberg^a, Brigitte von Rechenberg^a, Marc Bohner^{b,*},
Sonja Grünenfelder^b, G Harry van Lenthe^c, Ralph Müller^c, Beat Gasser^b,
Robert Mathys^b, Gamal Baroud^d, Jörg Auer^a

^aMusculoskeletal Research Unit (MSRU), Equine Hospital, University of Zurich, Winterthurerstrasse 260, CH 8057 Zurich, Switzerland

^bDr Robert Mathys Foundation, Bischmattstrasse 12, CH 2544 Bettlach, Switzerland

^cInstitute for Biomedical Engineering, University and ETH Zurich, Moussonstrasse 18, CH 8044 Zurich, Switzerland

^dFaculté de génie mécanique, Université de Sherbrooke, Sherbrooke, Canada J1K2R1

Received 22 March 2006; accepted 18 May 2006

Available online 21 June 2006

Abstract

The goal of the present study was to assess the effect of macropore size on the in vivo behavior of ceramic scaffolds. For that purpose, β -tricalcium phosphate (β -TCP) cylinders with four different macropore sizes (150, 260, 510, and 1220 μm) were implanted into drill hole defects in cancellous bone of sheep and their resorption behavior was followed for 6, 12 and 24 weeks. The scaffolds were evaluated for biocompatibility, and new bone formation was observed macroscopically, histologically and histomorphometrically. Histomorphometrical measurements were performed for the whole defect area and for the area subdivided into three concentric rings (outer, medial, and inner ring). All implants were tolerated very well as evidenced by the low amount of inflammatory cells and the absence of macroscopic signs of inflammation. Resorption proceeded fast since less than 5% ceramic remained at 24-week implantation. Hardly any effect of macropore size was observed on the in vivo response. Samples with an intermediate macropore size (510 μm) were resorbed significantly faster than samples with smaller macropore sizes (150 and 260 μm). However, this fast resorption was associated with a lower bone content and a higher soft tissue content. At 12 and 24 weeks, the latter differences had disappeared. Bone was more abundant in the outer ring than in the rest of the blocks at 6 weeks, and in the outer and medial ring compared to the inner ring at 12 weeks.

© 2006 Elsevier Ltd. All rights reserved.

Keywords: β -tricalciumphosphate; Pore size; Resorption; Bone; Biocompatibility; Ingrowth

1. Introduction

Bone substitutes have received much attention in the last four decades [1–19], in particular in a recent review [20]. Despite these efforts, it is still not clear what an optimal geometry for these bone substitutes should be except that blocks should contain interconnected macropores and that the macropore diameter and the macropore interconnections should be larger than 50–100 μm in diameter [1–20]. In fact, various optima might exist depending on the purpose of the bone substitute. For example to culture cells on- and in a porous blocks, block permeability should

probably be very high [21], i.e. macropores should be as large and interconnected as possible [22]. In vivo, smaller macropores (macropore size close to 50–800 μm) appear to be more adequate in terms of bone ingrowth and/or ceramic resorption [1–20].

Recently, Bohner and Baumgart [23] proposed a theoretical approach to determine the macropore morphology minimizing the resorption time of a bone substitute with a cell-mediated resorption (typically a ceramic bone substitute). Contrary to previous studies, this work was purely theoretical. Interestingly, the model predicted for non or partly interconnected macroporous scaffolds an optimum macropore size in the range of 50–800 μm depending on the macroporosity volume fraction, the size of the implanted block and the diameter of the pore

*Corresponding author. Tel.: +41 32 6441413; fax: +41 32 6441176.

E-mail address: marc.bohner@rms-foundation.ch (M. Bohner).

interconnections. A decrease of the diameter of the pore interconnection or of the macroporosity volume fraction, or an increase of the size of the implanted block were expected to increase the macropore size at which the total resorption time was minimized. The comparison between the theoretical findings of Bohner and Baumgart [23] and *in vivo* data gathered on dense spherical/cylindrical bone substitutes showed a very good correlation. Unfortunately, the latter authors did not apply the model to results obtained on porous bone substitutes due to a lack of adequate experimental data.

In fact, there are plenty of studies looking at an optimum of macropore size [1–19] but these have only considered one or two macropore geometries at only one or two different times. Moreover, many studies have been devoted to poorly resorbable bone substitutes (e.g. hydroxyapatite) where the focus has been a fast bone ingrowth rather than a fast ceramic resorption. The study of Galois and Mainard [14] appears to be the exception even though the porous structures were not very well described.

As a result, a new animal study was conducted to look at the *in vivo* behavior of β -tricalcium phosphate (β -TCP) blocks with 4 macropore diameters (150, 260, 510 and 1220 μm) at three different implantation times (6, 12, and 24 weeks). The two specific aims of the study were: (i) to investigate histologically the effect of macropore size on the cellular response, and (ii) to investigate the effect of macropore size on the ceramic resorption, and bone ingrowth. For that purpose, macroscopical, radiological, histological and histomorphometrical analysis were performed.

2. Materials and methods

2.1. Blocks

The synthesis and characterization of the blocks has been described extensively in a previous publication [24]. Briefly, the blocks consisted of phase-pure β -TCP (as observed by X-ray diffraction). The samples were cylindrical with a diameter of 8 mm and a length of 13 mm. The microporosity (diameter smaller than 50 μm), macroporosity (diameter greater than 50 μm) and the total block porosity were close to 21%, 54% and 75% for all macropore sizes. Macropores were spherical and partly interconnected (about 2 interconnections per macropore [24]; Fig 1). Four mean macropore diameters were obtained depending on the synthesis conditions: 150, 260, 510 and 1220 μm . The latter sizes were measured optically [24]. Twenty-five percent lower values were obtained by analysing μCT results. The macropore size distribution was narrow and followed a normal distribution. The mean compressive strengths were all found in the range of 2.2–3.7 MPa without any significant effect of pore size. The blocks were delivered in a small syringe that could not only be used to aspirate liquids, but also to apply vacuum to the inner part of the syringe. This device was used to soak the blocks with blood before implantation.

2.2. Sheep

Nine adult female Swiss Alpine sheep (3–4 years of age with a body weight ranging from 64–75 kg) were used for the study, which was approved by the local Ethical Committee and veterinary authorities

(application number 176/2003). The sheep were examined for their state of health clinically and haematologically. Tetanus vaccine and an anthelmintic were administered. They were acclimatized to their new housing facilities for 2 weeks before surgery.

2.3. Scaffold location

The β -TCP cylinders were distributed randomly to eight predefined metaphyseal or epiphyseal locations in long bones of the sheep: left and right proximal humerus, proximal femur, proximal tibia, and distal femur [25]. Two samples of each macropore size were implanted per sheep. Three time groups were formed according to observation periods (6, 12 and 24 weeks), each group containing three animals (Table 1). So, a total of 6 samples of each macropore size was implanted at each observation period.

2.4. Anaesthesia

Anaesthesia was performed as previously described by Theiss et al [25]. Briefly, sheep were sedated with medetomidine (5 $\mu\text{g}/\text{kg}$ i.m., DomitorTM, Orion Animal Health, Finland) served as pre-medication and anaesthesia was induced with diazepam (0.1 mg/kg, ValiumTM, Roche Pharama, Switzerland) and ketamin (2 mg/kg, Narketan 10TM, Chassot GmbH, Germany). Anaesthesia was maintained by isoflurane-oxygen inhalation (FORENETM, Abbot AG, Switzerland).

2.5. Medication

Prior to anaesthesia 30.000 IU/kg aqueous penicillin G (Grünenthal 10 Mega[®], Grünenthal GmbH, Aachen, Germany) and 6 mg gentamicin sulfate (G. Streuli Ag, Uznach, Switzerland) were administered via a jugular catheter. Perioperative analgesic and anti-inflammatory therapy was provided by 0.01 mg/kg buprenorphine (Temgesic[®], Essex Chemie AG, Luzern, Switzerland) intramuscularly and 4 mg/kg carprofene (Rimadyl[®], Pfizer AG, Zurich, Switzerland) intravenously. Anti-inflammatory and antibiotic medication was maintained for 4 days after surgery.

2.6. Surgery

The sheep were placed in lateral recumbency. Aseptic preparation of the surgical site was performed routinely as formally described [25]. After implanting all samples from one side the animals were rotated onto the other side for the same procedure. A small lateral approach with stab incision was made directly over the location except for the tibia, which was approached from the medial side. The fascia was incised and a blunt dissection was performed down to the bone. The drill holes were created with a 8.00 mm drill with a stop at 13 mm length (KaVo INTrASurg 500[®], KaVo Dental AG Biberach, Germany). After drilling, the holes were flushed and cleaned with saline (0.9%) and a sterile swab. The samples were delivered sterile in a syringe that helped to infiltrate the calcium cement cylinders with blood supplied by the same sheep. Blood infiltration was achieved by creating a vacuum within the syringe cylinder. Afterwards the cylinders were carefully inserted into the drill holes manually. Overlying soft tissue was closed in layers with resorbable suture (Vicryl[®] 2/0 Johnson & Johnson, Brussels, Belgium) and skin staples were used to close the skin (Davis and Geck Appose ULCr, B. Braun Aesculap AG, Tuttlingen, Germany). The staples were removed 10 days after surgery. In the time between surgery and slaughter the animals were allowed to roam freely on the pasture.

2.7. Macroscopic evaluation

The bones were harvested immediately after slaughter. Macroscopical appearance was assessed with regard to inflammatory reaction and overgrowth of the neighboring tissue according to a score system. Inflammatory reaction assessed by looking at the color of the implant

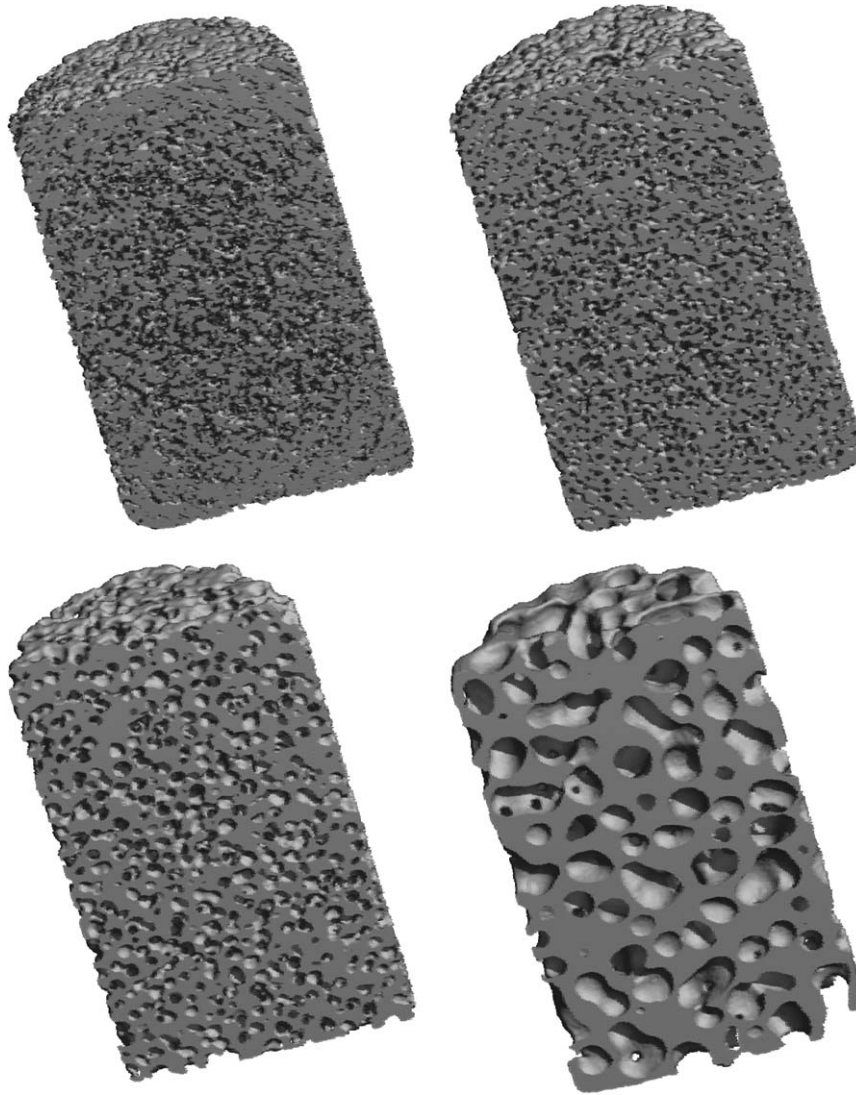


Fig. 1. Typical μ CT scans of the four different blocks.

Table 1
Macropore size and group distribution

Observation period	Sheep	HPL	FPL	FDL	TPL	HPR	FPR	FDR	TPR
06 weeks	864	C	A	B	D	A	C	D	B
	865	D	B	C	A	B	D	A	C
	866	A	C	D	B	C	A	B	D
12 weeks	861	A	C	D	B	C	A	B	D
	862	B	D	A	C	D	B	C	A
	863	C	A	B	D	A	C	D	B
24 weeks	858	C	A	B	D	A	C	D	B
	859	D	B	C	A	B	D	A	C
	860	B	D	A	C	D	B	C	A

HPL: left proximal humerus, FPL: left proximal femur, FDL: left distal femur, TPL: left proximal tibia.

HPR: right proximal humerus, FPR: right proximal femur, FDR: right distal femur, TPR: right proximal tibia.

A: 150 μ m, B: 260 μ m, C: 510 μ m, D: 1220 μ m.

site: 0 = none, 1 = mild, 2 = moderate (reddening). Macroscopical evaluation: 0 = none, 1 = partly covered, 2 = covered by a thin layer, 3 = no detectable implant.

2.8. Radiographs

Radiographs of each bone were taken in frontal (0°) and lateral (90°) views after dissecting the bones from all soft tissue. The adjacent bone was evaluated for signs of sclerosis or osteolysis. The density of each sample was compared to the density of the adjacent bone (Faxitron[®] X-ray System, Hewlett & Packard, Oregon, USA).

2.9. Histology and histomorphometry

Histological thick (30–40 µm) and thin (5 µm) sections were prepared as described by Theiss et al [25]. Basically, all sections were made perpendicular to the long side of the cylinders in the centre of the defect. The thick sections were surface stained with toluidine blue, whereas the thin sections were deplastified and stained with toluidine blue and von Kossa/Mc Neal's Tetrachrome.

Thin sections were used for the histological qualitative and semiquantitative evaluation. The quality of new bone formation, ceramic resorption, and occurrence of soft tissue and inflammatory cells was described. The character and amount of the cells found in three fields of vision of the whole implant area of each section (at magnification 200) were evaluated, supported by a specifically developed scoring system (Leica DMR[®]; Leica Microsystems Wetzlar GmbH, Wetzlar, Germany). The cells were: giant cells linked to the ceramic (score: 0 for none, 2 for more than 4 cells), giant cells linked to bone (score: 0 for none, 2 for more than 4 cells), macrophages (score: 0 for none, 1 for up to 2 macrophages, 2 for more than 2 macrophages), plasma cells (score: 0 for none, 1 for up to 2 cells, 2 for more than 2 cells) and granulocytes (score: 0 for none, 1 for up to 2 cells, 2 for more than 2 cells). Noteworthy, leukocytes and granulation tissues which are typically present in the phases of inflammation could not be found and hence their presence was not assessed. Remodelling was assessed by counting the number and the orientation of osteoblasts (0: none or few osteoblasts that were not aligned along bone margins; 1: few aligned cells; 2: lots of aligned cells).

Thick sections were used for histomorphometrical evaluation in combination with an image-analysis system comprising of a microscope and three software programs (Leica IM 1000[®], Leica Qwin[®] and Adobe Photoshop 7[®]). The areas in the defect occupied by either bone or ceramic were stained manually to ensure accurate detection during the measurement. The program detected the area surrounding the defect as well as three of the four phases present in the defect. The three phases were newly formed bone, remaining ceramic and an undefined phase called "holes". This phase corresponds to all empty areas (resulting from the histological processing method) within the observed domain. Even though most of the former material consisted of soft tissue, e.g. bone marrow, it could also be possible that these areas contained fair amounts of ceramic remnants or newly formed bone, as observed in former studies [25–27]. The fourth phase, fibrous tissue, was determined by the difference between the total of all three other phases and 100%. In the present document, the third and fourth phase are considered as a unique phase denominated "soft tissue". Furthermore the area of the defect was divided into three circular areas with constantly increasing radius: inner ring (IR), medial ring (MR) and outer ring (OR) (Fig 2). By this method results were calculated for the whole implant area and for every single area to assess the progression of bone ingrowth and resorption. Results were given in mm² for the whole sample area and each sub-area.

2.10. Statistics

A factorial analysis of variance (ANOVA) with Bonferroni/Dunn Post-Hoc test (StatView 5.1[®], Abacus Inc., Berkeley, California) was carried out on the semi-quantitative (cell number and type) and histomorpho-

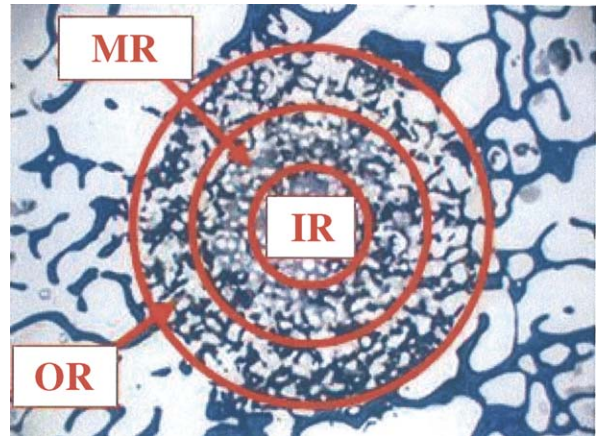


Fig. 2. Defect area subdivided into ring areas: outer ring (OR), medial ring (MR) and inner ring (IR).

metry (bone, ceramic and soft tissue content) results. A student *t*-test was also applied on the data to assess (i) the effect of macropore size at each of the three implantation times and the three locations, and (ii) the effect of location (OR, MR and IR) for each macropore size and implantation time. Results were considered to be significant at $p < 0.01$.

3. Results

3.1. Surgeries

All surgeries were performed without complications. The samples could be easily infiltrated with blood using the vacuum system and all samples were introduced into the defects without being damaged. All sheep recovered well and showed no signs of lameness within the following 10 days until they had their skin staples removed and were sent on the pasture from where all sheep returned healthy before slaughter.

3.2. Macroscopical evaluation

No significant differences of macroscopical appearance and inflammatory reaction could be found between the different macropore sizes. The inflammatory response increased from week 6 (mild or moderate inflammation in 37.5% of the defects) to week 12 (63.6% of the defects) and then disappeared at week 24 (Table 2). Visually, it was difficult to locate the blocks which is a positive sign. The percentage of undetectable blocks steadily increased from week 6 (20.8%) to week 12 (70.8%) and week 24 (100%; Table 3).

3.3. Radiological evaluation

The β -TCP scaffolds were clearly detectable at 6 weeks due to the higher radio density of the β -TCP in comparison to the adjacent bone. Slightly more radiodense zones with mild sclerosis of the adjacent bone were present after 6 weeks. After 12 weeks detection of the implants was more

Table 2
Macroscopical evaluation of inflammatory signs (reddening)

Observation period	None (%)	Mild (%)	Moderate (%)
6 weeks	62.5	20.8	16.7
12 weeks	33.4	37.5	26.1
24 weeks	100	0	0

Table 3
Macroscopical evaluation of soft tissue growth over the implant

Observation period	None (%)	Partly covered (%)	Covered by a thin layer (%)	Undetectable (%)
06 weeks	8.3	37.5	33.3	20.8
12 weeks	0.0	0.0	29.1	70.8
24 weeks	0.0	0.0	0.0	100

difficult and bone sclerosis was less obvious compared to earlier dates. After 24 weeks the location of the implants could only be guessed by interpretation of the trabecular pattern of the bone, since the difference in radio density could not be detected anymore. More material could be detected on microradiographs.

3.4. Qualitative histology

In the following text the four different macropore sizes will be referred to as A–D as shown in Table 1. Moreover, samples with the four macropore sizes will be called A, B, C, or D samples, respectively. With the toluidine blue staining, the location of the defect after 6 weeks implantation was clearly visible either on the thick or the thin sections (Figs 3 and 4). The adjacent trabecular pattern showed increased remodelling around the implant and new bone formation extended to the implant area. The macropores contained loose connective tissue with spindle-shaped cells. Small insular-like patches of dense deep blue matrix with osteocyte-like cells trapped within lacunae were more frequent towards the centre. These islands were partly seamed with dense osteoid of a lighter blue with cubical-shaped osteoblast-like cells lining them. Large multinuclear cells either connected to ceramic or new bone were also dominant towards the centre (Fig 5). Soft tissue emerged throughout the entire implant area in irregular patches. Inflammatory cells were rarely seen except for a few macrophages. After 12 weeks, new bone was detected in all areas even though the most intense remodelling characterized by the presence of osteoblasts and osteoid seams was seen at the periphery. Bone patches started to fuse displacing the ceramic and soft tissue. Few macrophages, plasma cells and granulocytes were dispersed in the soft tissue. After 24 weeks, the defect margins were difficult to recognize. The newly formed trabecula were slightly more irregular compared to normal bone. Only in

the centre residues of the implant were present, partly engulfed by new bone. Osteoblast-like cells were rarely seen in the centre and if so, they were much flatter than at 12 weeks.

3.5. Semi-quantitative histology

No statistically significant differences at $p < 0.01$ could be found between the various macropore sizes regarding remodelling and cell types (Table 4). The only significant effect at $p < 0.01$ was a decrease of the ceramic-linked giant cell population from week 6 to 24.

3.6. Histomorphometry

The resorption of the ceramic proceeded very rapidly in the first weeks of implantation: at 6 weeks, almost 80% of the ceramic had been resorbed (Table 5, Fig 6(a)). Later on, resorption took place at a slower pace. At 24 weeks, less than 5% of the total surface area was occupied by the bone substitute. Bone formation appeared to be delayed compared to ceramic resorption, because it took place at an almost constant rate for 12 weeks (Fig 6(b)). No large changes were then seen beyond 12 weeks. The soft tissue fraction (= total of fibrous tissue and hole content) remained approximately constant throughout the investigated period even though a maximum was observed at 6 weeks (Fig 6(c)).

Statistically, the ANOVA analysis revealed a significant difference of bone content between 6 and 12 weeks, and of ceramic content between 12 and 24 weeks. However, there was no effect of pore size. The student *t*-test showed some significant differences between the various pore sizes (Table 5 and 6). At 6 weeks, C samples had significantly less ceramic and more soft tissue than samples A and B. C samples had also less bone than A, B, and D samples, but only at $p < 0.016$, 0.015 and 0.017, respectively. At 24 weeks, A samples had significantly more ceramic than B samples (at $p < 0.01$). Overall, there was no significant effect of macropore size on bone, ceramic, or soft tissue fraction.

When the histomorphometrical results were analyzed separately in the three zones (OR, MR and IR; Fig 2), similar results were obtained (Table 7). The only two new aspects were the presence at 24 weeks of significantly more resorption in B samples compared to A samples (MR), and more bone in B samples compared to A samples (IR).

When looking at the difference between the results obtained in the various rings (e.g. bone content in the OR and MR), many significant results were found (using the student *t*-test; Table 8), but only at 6 and 12 weeks. Peculiarly, the soft tissue content generally increased, whereas the ceramic content generally decreased when moving from the outside to the inside (from OR to IR). The bone content was almost always larger in the OR than in the MR and IR at 6 weeks, and in the OR and MR compared to the IR at 12 weeks.

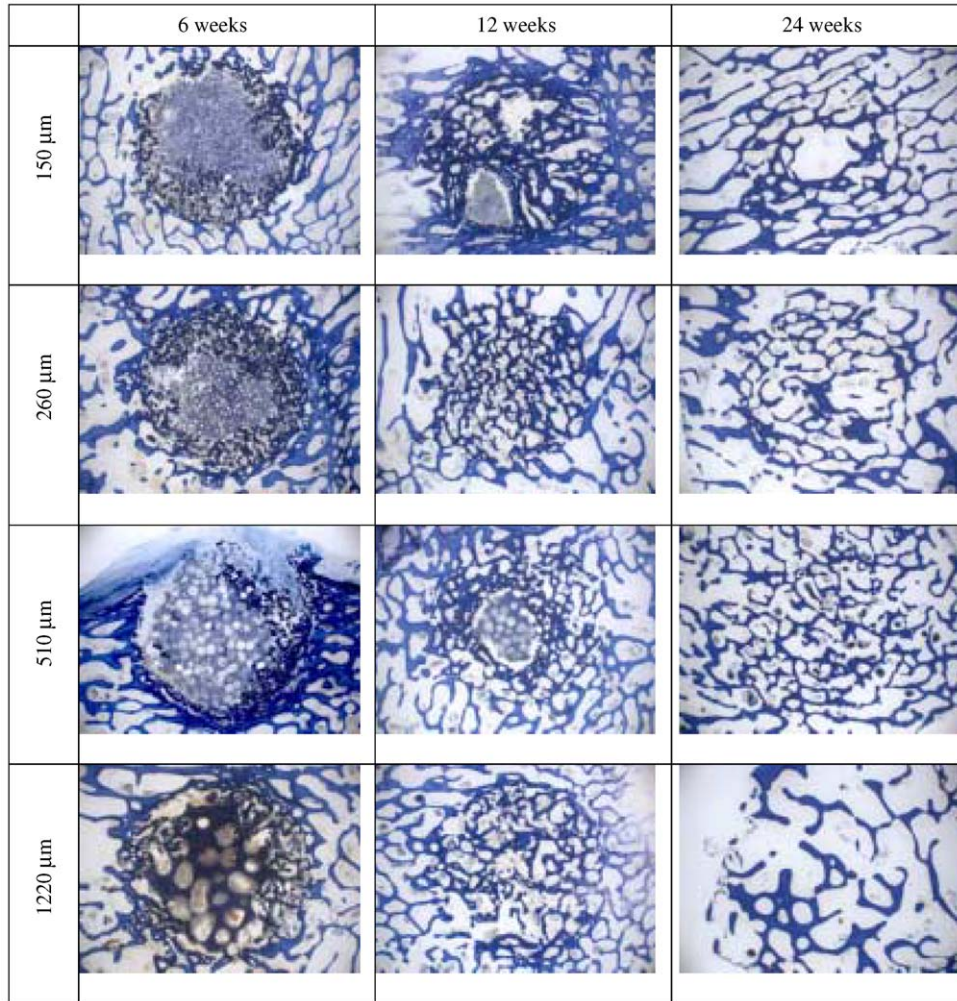


Fig. 3. Histological appearance of the thick sections after toluidine blue staining. From top to bottom: pore diameter of 150, 260, 510 and 1220 μm . From left to right: implantation time of 6, 12 and 24 weeks.

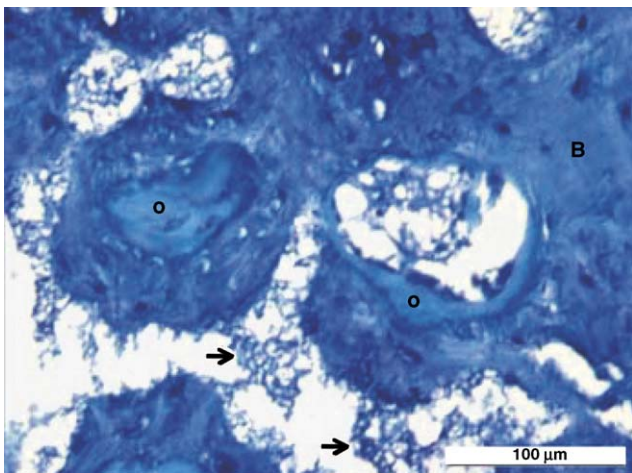


Fig. 4. Osteoid (O) and new bone (B) has formed in the former pores. Ceramic remnants (arrows) are found in the space between. Pore size A after 6 weeks at magnification 400 (toluidine blue staining).

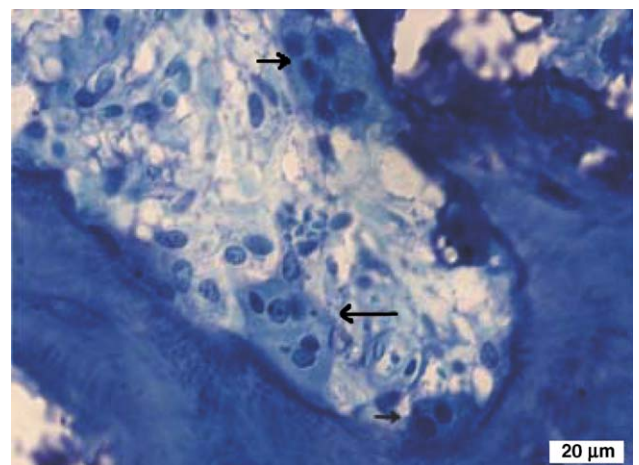


Fig. 5. Giant cells attached to newly formed bone (arrows), pore size A after 6 weeks at magnification 400 (toluidine blue staining).

Table 4
Semi-quantitative analysis of the cellular content of the implants

Observation period	Pore diameter (µm) A: 150 B: 260 C: 510 D: 1220	Remodelling 0: none 1: few 2: much	Bone-linked giant cells 0: none 2: over 4	Ceramic-linked giant cells 0: none 2: over 4	Macrophages 0: none 1: up to 2 2: over 2	Plasma cells 0: none 1: up to 2 2: over 2	Granulocytes 0: none 1: up to 2 2: over 2
06 weeks	A	0.9±0.8	0.4±0.6	0.7±0.8	0.6±0.8	0.2±0.6	0.3±0.6
	B	1.3±0.8	0.2±0.4	0.9±0.8	0.6±0.6	0.1±0.2	0.1±0.4
	C	1.1±0.9	0.6±0.6	0.5±0.7	0.7±0.8	0.2±0.6	0.4±0.7
	D	1.3±0.8	0.2±0.6	1.0±0.5	1.0±0.8	0.1±0.3	0.3±0.7
12 weeks	A	1.4±0.7	0.3±0.5	0.5±0.5	1.1±0.9	0.4±0.7	0.3±0.5
	B	1.2±0.8	0.3±0.5	0.5±0.6	0.7±0.9	0.1±0.3	0.2±0.4
	C	1.3±0.7	0.1±0.2	0.4±0.6	0.8±0.8	0.4±0.8	0.0±0.0
	D	1.5±0.5	0.2±0.4	0.2±0.5	0.8±0.8	0.1±0.3	0.1±0.5
24 weeks	A	1.1±0.7	0.3±0.4	0.0±0.0	0.7±0.9	0.1±0.2	0.2±0.6
	B	1.1±0.8	0.3±0.4	0.1±0.2	0.9±0.8	0.1±0.3	0.1±0.3
	C	0.9±0.8	0.1±0.2	0.1±0.2	0.3±0.5	0.1±0.2	0.1±0.3
	D	1.1±0.9	0.4±0.5	0.2±0.5	0.5±0.6	0.1±0.2	0.1±0.3

Table 5
Means of the histomorphometrical analysis subdivided into rings

Observation period	Phase	Pore size	OR			MR			IR			Total
			Av	SD	%	Av	SD	%	Av	SD	%	
06 weeks	Bone matrix	A	4.12	1.20	14.7	1.25	0.88	7.5	0.29	0.21	5.2	5.66
		B	5.03	2.34	18.0	1.26	0.79	7.5	0.16	0.22	3.0	6.45
		C	2.51	1.18	9.0	0.83	0.52	5.0	0.21	0.17	3.8	3.55
		D	5.38	2.99	19.2	1.36	1.10	8.1	0.23	0.30	4.3	6.97
	Ceramic	A	3.93	1.49	14.0	1.89	1.07	11.3	0.15	0.25	2.7	5.97
		B	2.67	1.05	9.5	2.46	0.82	14.7	0.80	0.71	14.6	5.93
		C	2.31	1.33	8.3	0.82	0.68	4.9	0.10	0.10	1.8	3.23
		D	2.17	1.53	7.7	1.64	0.69	9.8	0.39	0.34	7.1	4.20
	Fibrous tissue	A	19.97	2.48	71.3	13.60	1.36	81.2	5.03	0.29	92.0	38.60
		B	20.32	2.69	72.5	13.02	1.49	77.8	4.51	0.90	82.4	37.84
		C	23.19	1.34	82.8	15.09	0.87	90.1	5.16	0.24	94.4	43.44
		D	20.47	3.52	73.1	13.74	1.44	82.1	4.85	0.57	88.6	39.05
12 weeks	Bone matrix	A	9.58	3.37	34.2	4.31	1.55	25.7	0.60	0.43	11.0	14.49
		B	9.38	2.29	33.5	4.57	1.09	27.3	0.96	0.46	17.6	14.91
		C	9.46	1.70	33.8	4.26	1.29	25.5	0.86	0.41	15.8	14.59
		D	8.73	2.56	31.1	3.87	1.03	23.1	0.89	0.52	16.3	13.49
	Ceramic	A	1.72	0.97	6.1	1.72	0.85	10.3	0.58	0.42	10.6	4.02
		B	2.03	1.60	7.3	1.88	0.89	11.2	0.65	0.30	11.8	4.56
		C	1.56	0.68	5.6	1.65	0.51	9.8	0.86	0.39	15.7	4.07
		D	1.97	1.30	7.0	1.62	0.90	9.7	0.54	0.37	9.8	4.12
	Fibrous tissue	A	16.71	3.55	59.7	10.71	1.29	64.0	4.29	0.74	78.4	31.71
		B	16.60	2.95	59.3	10.29	1.14	61.5	3.86	0.45	70.6	30.76
		C	16.99	1.56	60.6	10.83	1.07	64.7	3.74	0.61	68.5	31.57
		D	17.32	2.75	61.8	11.25	1.44	67.2	4.04	0.76	73.9	32.61
24 weeks	Bone matrix	A	6.28	3.15	22.4	4.06	1.96	24.3	1.00	0.56	18.3	11.35
		B	10.05	4.28	35.9	6.13	3.11	36.6	1.99	0.87	36.3	18.17
		C	7.74	2.30	27.6	3.60	0.98	21.5	1.26	0.79	23.0	12.59
		D	7.30	2.57	26.1	4.49	1.74	26.8	1.49	0.67	27.2	13.28
	Ceramic	A	0.74	0.40	2.6	0.63	0.49	3.8	0.18	0.12	3.3	1.55
		B	0.39	0.37	1.4	0.14	0.21	0.9	0.06	0.09	1.1	0.59
		C	0.66	0.89	2.3	0.60	0.75	3.6	0.25	0.30	4.5	1.50
		D	0.84	0.71	3.0	0.35	0.17	2.1	0.08	0.08	1.4	1.26
	Fibrous tissue	A	21.00	3.16	74.9	12.05	1.74	72.0	4.28	0.58	78.4	37.33
		B	17.61	4.26	62.9	10.47	3.03	62.5	3.43	0.86	62.7	31.50
		C	19.62	2.11	70.0	12.54	0.92	74.9	3.97	0.84	72.6	36.12
		D	19.88	2.76	71.0	11.90	1.81	71.1	3.90	0.73	71.4	35.68

Total area = 50.2 mm²; OR = outer ring area (28.0 mm²), MR = medial ring (16.7 mm²), IR = inner ring (5.5 mm²). The average surface area of each phase (e.g. bone) is indicated either in mm² (column "Av") or in percent of the total surface area (column "%"). The standard deviation of the surface area (column "SD") is expressed in mm². The initial ceramic fraction is assumed to be 46% (macroporosity = 54% [24]).

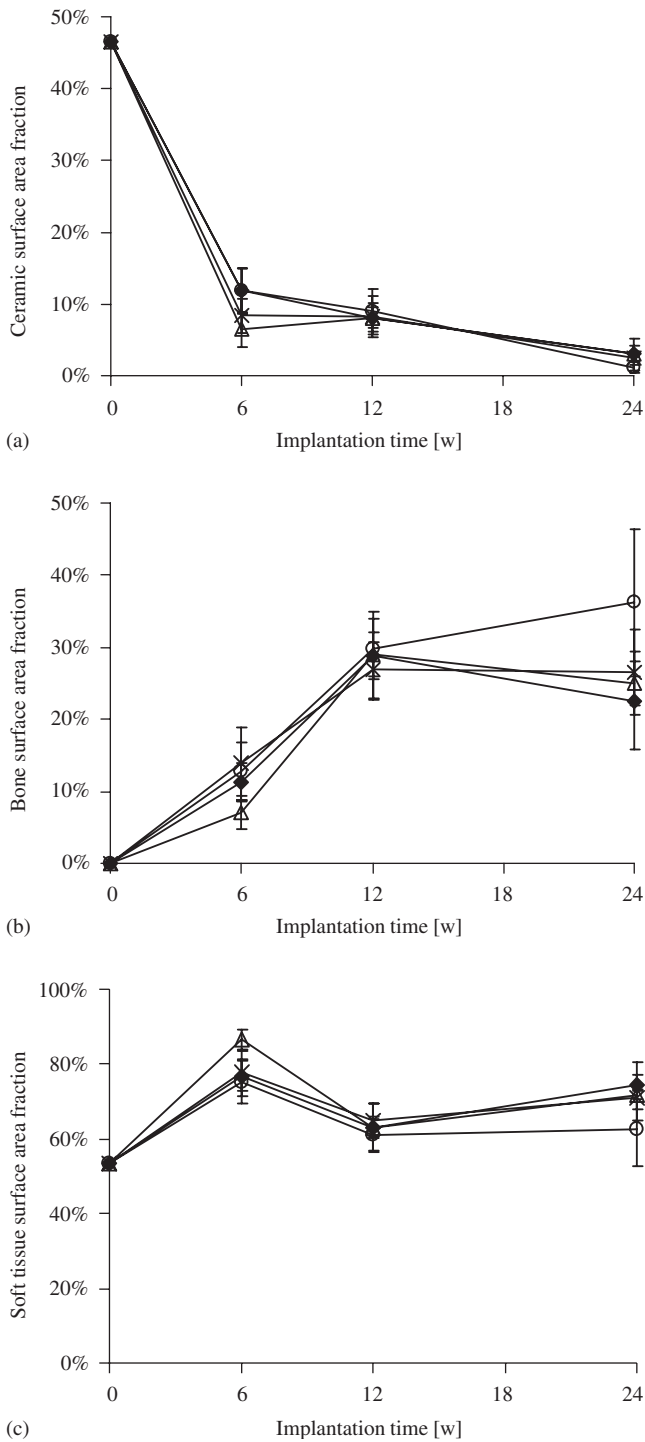


Fig. 6. Histomorphometrical results: evolution of the (a) ceramic, (b) bone, and (c) soft tissue in the bone defects as a function of block pore size. The values are expressed in surface fraction. Pore size: (◆) 0.15 mm; (○) 0.26 mm; (△) 0.51 mm; (×) 1.22 mm. The error bars correspond to a 95% confidence interval on the mean.

4. Discussion

4.1. General considerations

The specific aims of this study were twofold: (i) investigate histologically the effect of macropore size of a

Table 6

Qualitative results and significant differences at $p < 0.01$ when looking at the effect of pore size on the ceramic, bone and soft tissue content in the whole implantation area

Implantation time	Ceramic	Bone	Soft tissue
6 weeks	A > C* B > C*	—	A < C* B < C*
Order	A > B > D > C	D > B > A > C	C > D > A > B
12 weeks	—	—	—
Order	B > D > C > A	B > C > A > D	D > A > C > B
24 weeks	A > B*	—	—
Order	A > C > D > B	B > D > C > A	A > C > D > B
Overall	—	—	—

Macropore diameters: A: 150; B: 260; C: 510; D: 1220 μm . The sign “>” means “more of”, e.g. at 6 weeks there is significantly more bone left for pore size B compared to pore size C at $p < 0.01$: B > C. The order of the results is also indicated at 6, 12 and 24 weeks even though only few differences are significant at $p < 0.01$. For example, at 6 weeks, the fraction of ceramic remnants was in the following decreasing order: A, B, D and C (written: A > B > D > C). However, only the difference between A and C, as well as between B and C was significant at $p < 0.01$. The star (*) means that the difference is significant at $p < 0.01$.

Table 7

Qualitative results and significant differences at $p < 0.01$ when looking at the effect of pore size on the ceramic, bone and soft tissue content in the three sub-implantation areas, OR, MR and IR

Implantation time	Location	Ceramic	Bone	Soft tissue
6 weeks	OR	A > D	A, B, D > C	A, B < C
	MR	A, B, D > C	—	A, B < C
	IR	B > C	—	—
12 weeks		—	—	—
24 weeks	OR	—	—	—
	MR	A > B	—	—
	IR	—	A < B	—

Macropore diameters: A: 150; B: 260; C: 510; D: 1220 μm . The sign “>” means “more of”, e.g. at 6 weeks and in the outer ring (OR), there is more ceramic left for pore size A compared to pore size D: A > D.

ceramic bone substitute on its cellular response, and (ii) investigate the effect of macropore size on its resorption, and on the bone ingrowth. For these purposes, cylinders of 13 mm length and 8 mm in diameter were implanted into drill hole defects in cancellous bone of sheep. The specimens were harvested after 6, 12 and 24 weeks and evaluated macroscopically, radiographically and histologically. Histological evaluation was performed qualitatively, semiquantitatively and histomorphometrically. A more general aim of the study was to gather reliable data to apply the in vivo resorption model proposed by Bohner and Baumgart [23]. For that purpose, implanted blocks were extensively characterized before and after implantation. The results of the pre-implantation characterizations

Table 8

Qualitative results and significant differences at $p < 0.01$ when looking at the effect of location (OR, MR and IR) on the ceramic, bone and soft tissue content at the three implantation times and for the 4 pore sizes

Implantation time	Pore size	Ceramic	Bone	Soft tissue
6 weeks	A	OR, MR > IR	OR > MR, IR	OR < MR < IR
	B	OR < MR	OR > MR, IR	—
	C	OR > IR	OR > IR	OR < MR, IR
	D	—	OR > MR, IR	OR < IR
12 weeks	A	—	OR, MR > IR	OR, MR < IR
	B	—	OR, MR > IR	OR, MR < IR
	C	OR < MR, IR	OR > MR > IR	—
	D	—	OR > IR	—

Macropore diameters: A: 150; B: 260; C: 510; D: 1220 μm . The sign “>” means “more of”, e.g. at 6 weeks, there is more ceramic left in the outer and medial ring compared to the inner ring: OR, MR > IR. No significant differences were found at 24 weeks.

were published recently [24]. The post-implantation characterizations performed with micro-computed tomography (μCT) and the application of the model on the collected data are out of the scope of the present study and will be the subject of a future publication.

4.2. Experimental conditions

β -TCP was chosen as a model due to its biocompatibility, osteoconductivity and cell-mediated resorbability. A biologically more relevant calcium phosphate such as (precipitated) carbonated apatite could have been considered but was finally not selected due to its difficult synthesis and low mechanical properties (absence of sintering). Since the resorption model of Bohner and Baumgart [23] applies to all bone substitutes whose resorption is cell-mediated (like β -TCP), the conclusions retrieved from the comparison between the resorption model and the experimental data obtained with β -TCP should be applicable to other bone substitutes such as carbonated apatite.

Four macropore sizes and three different implantation times were selected to provide enough data points to apply the resorption model of Bohner and Baumgart [23] at a later time point. The blocks were synthesized according to the so-called calcium phosphate emulsions [28] in a similar fashion to the production of a commercial product called chronOSTM (Synthes, Bettlach, Switzerland). This method has four advantages: (i) the macropores size distribution is narrow [24]; (ii) the macropore size can be easily changed (with a change of emulsifier concentration) [28]; (iii) the macropore structure (interconnections, distribution within the scaffold) is almost independent of the selected macropore size [24]; and (iv) the ceramic blocks obtained after sintering are highly microporous hence enabling not only an easy machining process but also surgeons to change the block shape with a scalpel. However, the porous structure cannot be described by a few geometrical parameters (e.g. macropore size and distance between macropores), since the macropore distribution is random. Moreover, the interconnection size cannot be perfectly controlled as with other methods [15,29].

The sheep used as experimental animal in this study was considered to be appropriate since on the one hand many attributes of ovine cancellous bone are similar to those of human bone [30,31]. On the other hand, their suitability for drill hole defects had been tested and proven in former studies [25–27,32]. All sheep used in this study belonged to the same breed and sex and were nearly of the same age (3–4 years) and body weight (64–75 kg) to provide a minimum of standardization. To satisfy the ethical claim for few experimental animals and simultaneously collect enough data for a statistical analysis each of the nine sheep received eight implants, summing up to 72 implants altogether. Macropore sizes were distributed randomly to spread the varying influences of the specific locations.

The three implantation times selected here were taken based on the experience gathered with a resorbable calcium phosphate cement containing a large β -TCP fraction [25–27,32]. Unfortunately, the present results indicate that the last implantation time (24 weeks) was too long since only small changes were observed between 12 and 24 weeks. Retrospectively, it would have been better to select an implantation time of 3, 6 and 12 weeks, in a time frame during which large changes occur.

4.3. Application

In none of the scaffolds areas entirely abandoned of cells could be observed as described by Rose [13] and Kühne [7]. In the short period of time between infiltration and implantation a possible dissolution of the implant did not occur and all samples could be administered easily.

4.4. Sample extraction

After slaughter cubes of 20 × 20 mm size were cut guided by radiographs taken of the bones from two different views. In a few cases the defect area was hit or cut very close to the edge. All parts of a harmed implant were later measured and investigated as one scaffold to prevent this source of error from impairing results.

For two reasons no further investigation was performed on the radiographs and microradiographs taken post mortem: The first being that X-rays were developed digitally. Minimal changes in bone density and thickness led to differing results, in spite of all attempts to standardize the method. Pictures were corrected automatically according to the program chosen in the X-ray equipment and different results were obtained. The second reason was that after 6 weeks the radio densities of β -TCP and of the adjacent bone were already very similar and became more and more alike the longer the implant dwelled in the animal. The same problems occurred for the microradiographs. However, since the latter were taken from exactly the same sections, which later were grounded and stained, they were used to illustrate the ground sections. Without the distracting colors, the simple black and white pictures helped to determine the defect's margins and changes of the trabecular pattern of the adjacent bone and in the defect area itself.

All sections were cut out of the centre of the cylinder. One disadvantage of choosing one single location was that the ends of the cylinder were not taken into account. The centre was chosen because the most deficits concerning bone ingrowth and resorption were supposed to be found there. However, the fact that all sections stemmed from the same geometric location helped to standardize the method.

4.5. Histomorphometry

In the ground sections the area of the defect with the various phases was detected and stained manually with a software program. The method was based on the methods and experiences of former studies [25–27]. Due to the specific question of this study, the defect area was subdivided into three concentric zones (Fig 2). These zones did not refer to real areas in the ceramic blocks; they simply represented a gradation system.

The third phase detected by the histomorphometry program was the empty space in the implant area. This space was called “holes” because any former material had been removed during the histological preparation process. Even though it seems likely that most of the former material consisted of soft tissue, e.g. bone marrow, it could also be possible that these areas contained fair amounts of ceramic remnants or newly formed bone, which was often the case in former studies [25–27]. A detailed description of the cells found in thin slices of exactly the same areas (see semiquantitative and qualitative analysis) did not reveal a completely missing phase that would be easily associated with the holes. However, the space had to be detected and measured to be distinguishable from fibrous tissue. In the present document, it was decided to combine the “hole” and “fibrous tissue” fractions and call this new fraction the “soft tissue” fraction. This decision was supported by the results of μ CT investigations collected on implanted samples (data not presented and discussed here) that revealed similar values for the soft tissue fraction as the

values measured by histomorphometry. However, the statistical analysis of the results obtained in the various locations (OR, MR and IR) are unlogical (more ceramic remnants in OR than in IR, more soft tissue in IR than in OR) and suggest that the assumption done regarding the hole phase was perhaps not always correct.

4.6. Statistics

All evaluations had to undergo a factorial analysis of variance (ANOVA). By this method means of each evaluation level could be compared. In the semiquantitative analysis the distances from one score to another were chosen equidistantly. The set of statistics was completed by using Bonferroni/Dunn Post-Hoc test. Although great efforts were taken to optimize the statistical analysis all results have to be judged carefully due to the small number of experimental animals and expected variability in biological responses [33]. Since the ANOVA analysis did not reveal any significant effect of pore size, a second statistical analysis was performed. Instead of comparing variances (as in ANOVA), differences of means were compared (student *t*-test). A few hundred bilateral comparisons were performed due to the large number of factors, factor levels (4 pore sizes, 3 implantation times, 3 locations—OR, MR and IR), and responses (bone, ceramic and soft tissue content). At a significance level of $p < 0.01$, 1% of the few hundred comparisons should be significant at $p < 0.01$ due to simple probability rules. This has to be kept in mind when looking at the results.

4.7. Study goals

Based on a study from 1985, Klein et al. [34] suggested that β -TCP was neither biocompatible nor osteointegrative. These findings could not be confirmed. In this study the porous ceramic turned out to be biocompatible, resorbable, osteoconductive and osteointegrative as described before [35–42]. All implants bonded directly to bone and had no fibrous tissue detected at the interface. Bone spikes emerging into the implant were described as well as new bone formation on the macropore surfaces for all implants. Inflammatory cells were observed very rarely, and their presence was accredited to the healing process (Table 3). The same was true for the macroscopically detected inflammatory signs (Table 2).

Since the resorption behavior of a bone graft substitute is not only influenced by its chemical composition but also by its ultra structure this study was expected to reveal cases similar to those described by Hollinger et al. [43], who suggested that β -TCP resorption was unpredictable and occurred faster than new bone was formed. The latter results could be not be observed herein.

Macropore size influenced some of the biological responses such as ceramic resorption and bone ingrowth (Tables 6 and 7). The significance of these effects was sometimes very high (e.g. $p < 0.01$) but only small

differences were measured. All in all, resorption was significantly faster for C-sample (510 μm) compared to A and B samples (150 and 260 μm). This fast resorption was not correlated with a fast bone formation. On the contrary, bone formation was the slowest for that particular macropore size. However, this effect disappeared at 12 and 24 weeks implantation.

Differences of responses in the various locations (OR, MR and IR) were often significant, but only at 6 and 12 weeks. Two peculiar results were observed: the ceramic content decreased from the outside to the inside (10% surface area fraction in OR and MR, 7% in IR), whereas the soft tissue content increased from the outside to the inside. Based on the present data, it is not clear whether these results are real, or whether these results stem from an artefact of the measurements. The second solution appears to be the most likely. The ceramic is indeed more brittle than bone and hence could more easily drop off from the grinding section, particularly in a zone where no or little bone is present as it is the case in the IR at 6 weeks implantation. A zone in which a piece of ceramic fell off during processing is then counted to be part of the hole phase and hence of the soft tissue phase. A look at the collected data shows that the hole fraction increased from 24% (OR) to 25% (MR) and then 27% (IR) at 6 weeks. The extent of surface area change ($27-24 = 3\%$) has the same extent as that of ceramic content ($7-10 = -3\%$).

The bone fraction was found to be larger in the outer ring than in the medial and inner ring at 6 weeks, and in the outer and medial ring compared to the inner ring at 12 weeks. These results clearly indicate that bone ingrowth proceeds from the outside to the inside. The absence of significant effect at 24 weeks suggest that most of the ceramic resorption and healing process was finished at that time point.

In the scientific literature, the determination of an optimum of macropore size has been the topic of numerous publications [1–15]. Unfortunately, most studies have been focused on poorly resorbable bone substitutes where the focus was not ceramic resorption but bone ingrowth and bone formation. As a result, only very few studies describe an effect of macropore size on resorption. Moreover, the reported effects are contradictory: an increase of pore size is sometimes positive [5], sometimes negative [4,6], and sometimes without significant effect [2,14]. Interestingly, contradictory results can be expected from the resorption model of Bohner and Baumgart [23]. These authors predicted for a non or partly interconnected macroporous scaffold a minimum of the total resorption time at a macropore diameter in the range of 50–800 μm depending on the volume fraction of macroporosity, the size of the implanted block and the size of the pore interconnections. Therefore, depending on the experimental setting, a decrease or an increase in resorption time could be detected in the range of 50–800 μm . Noteworthy, the model predicted a decrease of the absolute effect of macropore

size with a decrease of the macroporosity volume fraction. In the present study and in the studies mentioned here above, the macroporosity volume fraction was in fact rather limited: 54% in the present study, 50% in [2], 60% in [4], 50% in [10], and 45% in [14], respectively (no indication of porosity in [5,6]). This could explain the difficulty in detecting an effect of macropore size. This finding could also be related to the observation of Lu et al. [10]: “in resorbable materials, pore density and interconnection density are more important than their size, contrary to unresorbable materials in which the sizes and the densities are equally important”.

The scientific literature does not provide a clear conclusion concerning an optimum of macropore size for bone ingrowth [20]. Some authors have found (i) an increase of the extent of bone ingrowth with an increase of pore size [1,5–7,9], (ii) a decrease of the extent of bone ingrowth with an increase of pore size [4,8,15], (iii) a maximum at an intermediate size [11,16,17], (iv) no effect at all [18,19] or (v) no effect provided the size of the pores is larger than 80 μm [14]. In the present study, no optimum was found, perhaps because bone ingrowth was already very advanced at the first implantation time (6 w).

In summary, the scientific literature reveals neither a clear optimum of pore size for implant resorption, nor for bone ingrowth. This absence of clear optimum could mean that parameters such as animal specie, block size, implant resorption, implant chemistry, implant topography, or pore fraction, could play such an important role that different optima are found in different experimental conditions. Another interpretation could be provided by the model of Bohner and Baumgart [23] which predicts that bone ingrowth should not be affected by pore size as long as the structure is fully interconnected and as long as the pore interconnections have a diameter larger than a minimum value thought to be close to 50 μm [10]. In a non-fully interconnected scaffold, bone ingrowth should be generally faster with larger macropores. However, bone formation has been shown to be promoted by the presence of calcium phosphate precipitates/particles due to a local excess of calcium ions [44,45]. So, bone ingrowth might be related to the rate of ceramic resorption which occurs faster with smaller pores. To summarize, the model of Bohner and Baumgart [23] predicts that apparently contradictory results should be obtained if the properties of the scaffold differ widely (e.g. non-fully interconnected or interconnected, non resorbable or resorbable, low or high porosity). This could well explain the apparently contradictory results obtained in the scientific literature.

In conclusion, the present study shows that all tested materials led to a very positive result as expressed by a fast transformation of β -TCP ceramic into bone. However, a fast resorption as seen for 510 μm pore samples was slightly detrimental to bone formation. A smaller (e.g. 260 μm) or a larger pore size (e.g. 1220 μm) might be more adequate in this animal model as bone substitute.

5. Conclusion

In the present study, β -TCP blocks of four macropore diameters (150, 260, 510, and 1220 μm) were implanted in metaphyseal or epiphyseal defects in sheep. The in vivo behavior was assessed macroscopically, radiologically, histologically and histomorphometrically. All blocks were found to be biocompatible, osteoconductive, and to lead to a fast turnover from ceramic to bone. Ceramic resorption occurred mainly in the first 6 weeks of implantation, whereas bone formation was observed during the first 12 weeks. Bone was more abundant in the outer ring than in the rest of the blocks at 6 weeks, and in the outer and medial ring compared to the inner ring at 12 weeks. The biological response to implantation was only marginally influenced by macropore size even though faster ceramic resorption and slower bone formation were found to occur in 510 μm pore samples compared to 150 and 260 μm pore samples.

References

- [1] Klawitter JJ, Hulbert SF. Application of porous ceramics for the attachment of load bearing internal orthopedic applications. *J Biomed Mater Res Symp* 1971;2(1):161–229.
- [2] Uchida A, Nade SM, McCartney ER, Ching W. The use of ceramics for bone replacement. A comparative study of three different porous ceramics. *J Bone Joint Surg Br* 1984;66(2):269–75.
- [3] Shimazaki K, Mooney V. Comparative study of porous hydroxyapatite and tricalcium phosphate as bone substitute. *J Orthop Res* 1985;3:301–10.
- [4] Egli PS, Müller W, Schenk RK. Porous hydroxyapatite and tricalcium phosphate cylinders with two different macropore size ranges implanted in the cancellous bone of rabbits. *Clin Orthop* 1988;232:127–38.
- [5] Daculsi G, Passuti N. Effect of macroporosity for osseous substitution of calcium phosphate ceramics. *Biomaterials* 1990;11:86–7.
- [6] Schliephake H, Neukam FW, Klosa D. Influence of pore dimensions on bone ingrowth into porous hydroxyapatite blocks used as bone graft substitutes. A histometric study. *Int J Oral Maxillofac Surg* 1991;20(1):53–8.
- [7] Kuhne JH, Bartl R, Frisch B, Hammer C, Jansson V, Zimmer M. Bone formation in coralline hydroxyapatite. Effects of pore size studied in rabbits. *Acta Orthop Scand* 1994;65(3):246–52.
- [8] Ishaug-Riley SL, Crane GM, Gurlek A, Miller MJ, Yasko AW, Yaszemski MJ, et al. Ectopic bone formation by marrow stromal osteoblast transplantation using poly(DL-lactic-co-glycolic acid) foams implanted into the rat mesentery. *J Biomed Mater Res* 1997; 36:1–8.
- [9] Gauthier O, Bouler J-M, Aguado E, Pilet P, Daculsi G. Macroporous biphasic calcium phosphate ceramics: influence of macropore diameter and macroporosity percentage on bone ingrowth. *Biomaterials* 1998;19:133–9.
- [10] Lu JX, Flautre B, Anselme K, Hardouin P, Gallur A, Descamps M, et al. Role of interconnections in porous bioceramics on bone recolonization in vitro and in vivo. *J Mater Sci Mater Med* 1999;10:1111–20.
- [11] Chang B-S, Lee C-K, Hong K-S, Youn H-J, Ryu H-S, Chung S-S, et al. Osteoconduction at porous hydroxyapatite with various pore configurations. *Biomaterials* 2000;21:1291–8.
- [12] Chu TMG, Orton DG, Hollister SJ, Feinberg SE, Halloran JW. Mechanical and in vivo performance of hydroxyapatite implants with controlled architectures. *Biomaterials* 2002;23:1283–93.
- [13] Rose FR, Cyster LA, Grant DM, Scotchford CA, Howdle SM, Shakesheff KM. In vitro assessment of cell penetration into porous hydroxyapatite scaffolds with a central aligned channel. *Biomaterials* 2004;25:5507–14.
- [14] Galois L, Mainard D. Bone ingrowth into two porous ceramics with different pore sizes: an experimental study. *Acta Orthop Belg* 2004;70:598–603.
- [15] Flautre B, Descamps M, Delecourt C, Blary MC, Hardouin P. Porous HA ceramic for bone replacement: role of the pores and interconnections—experimental study in the rabbit. *J Mater Sci Mater Med* 2001;12:679–82.
- [16] Götz HE, Müller M, Emmel A, Holzwarth U, Erben RG, Stangl R. Effect of surface finish on the osseointegration of laser-treated titanium alloy implants. *Biomaterials* 2004;25:4057–64.
- [17] Kuboki Y, Jin Q, Takita H. Geometry of carriers controlling phenotypic expression in BMP-induced osteogenesis and chondrogenesis. *J Bone Joint Surg* 2001;83:105–15.
- [18] Itälä AI, Ylänen HO, Ekholm C, Karlsson KH, Aro HT. Pore diameter of more than 100 μm is not requisite for bone ingrowth in rabbits. *J Biomed Mater Res (Appl Biomater)* 2001;58:679–83.
- [19] Ayers RA, Simske SJ, Bateman TA, Petkus A, Sachdeva RLC, Gyunter VE. Effect of nitinol implant porosity on cranial bone ingrowth and apposition after 6 weeks. *J Biomed Mater Res* 1999;45: 42–7.
- [20] Karageorgiou V, Kaplan D. Porosity of 3D biomaterial scaffolds and osteogenesis. *Biomaterials* 2005;26:5474–91.
- [21] Li S, De Wijn JR, Li J, Layrolle P, De Groot K. Macroporous biphasic calcium phosphate scaffold with high permeability/porosity ratio. *Tissue Eng* 2003;9(3):535–48.
- [22] Bohner M, Gasser B, Baroud G, Heini P. Theoretical and experimental model to describe the injection of a polymethylmethacrylate cement into a porous structure. *Biomaterials* 2003;24(16): 2721–30.
- [23] Bohner M, Baumgart F. Effects of geometrical factors on the resorption of calcium phosphate bone substitutes. *Biomaterials* 2004;25(17):3569–82.
- [24] Bohner M, van Lenthe GH, Gruenenfelder S, Hirsiger W, Evison R, Müller R. Synthesis and characterization of porous β -tricalcium phosphate blocks. *Biomaterials* 2005;26(31):6099–105.
- [25] Theiss F, Apelt D, Brand B, Kutter A, Zlinsky K, Bohner M, et al. Biocompatibility and resorption of a new brushite calcium phosphate cement. *Biomaterials* 2005;26(21):4383–94.
- [26] Kuemmerle JM, Oberle A, Oechslin C, Mueller J, Zlinsky K, Bohner M, et al. Assessment of the suitability of a new brushite calcium phosphate cement for cranioplasty—an experimental study in sheep. *J Cranio-maxillofacial Surg* 2005;33(1):37–44.
- [27] Oberle A, Theiss F, Bohner M, Müller J, Kästner SB, Frei C, et al. Nicht-keramische Kalziumphosphat-Zemente im Vergleich: Eine experimentelle Studie von Brushite vs. Hydroxylapatit Zement in vivo bei Schafen. *Schw Arch Tierheilkunde* 2005;147(11):482–90.
- [28] Bohner M. Calcium phosphate emulsions: possible applications. *Key Eng Mater* 2001;192–195:765–8.
- [29] Richart O, Descamps M, Liebetrau A. Macroporous calcium phosphate ceramics: optimization of the porous structure and its effect on the bone ingrowth in a sheep model. *Key Eng Mater* 2001;192–195:425–8.
- [30] Nunamaker DMV. Experimental models of fracture repair. *J Clin Orthop Relat Res* 1998;355:S56–65.
- [31] Sarkar MR, Wachter N, Patka P, Kinzl L. First histological observations on the incorporation of a novel calcium phosphate bone substitute material in human cancellous bone. *J Biomed Mater Res* 2001;58(3):329–34.
- [32] Apelt D, Theiss F, El-Warrak AO, Zlinsky K, Bettschart-Wolfsberger R, Bohner M, et al. In vivo behavior of three different injectable hydraulic calcium phosphate cements. *J Biomater* 2004; 25(7-8):1439–51.
- [33] Hüsler J. Statistische Prinzipien für medizinische Projekte: Verlag Hans Huber; 1996.

- [34] Klein CP, de Groot K, Driessen AA, van der Lubbe HB. Interaction of biodegradable β -whitelockite ceramics with bone tissue: an in vivo study. *Biomaterials* 1985;6(3):189–92.
- [35] Bauer TW, Smith ST. Bioactive materials in orthopaedic surgery: overview and regulatory considerations. *J Clin Orthop* 2002;395:11–22.
- [36] LeGeros RZ. Biodegradation and bioresorption of calcium phosphate ceramics. *J Clin Mater* 1993;14(1):65–88.
- [37] Albee F. Studies in bone growth: triple CaP as a stimulus to osteogenesis. *J Ann Surg* 1920;71:32–6.
- [38] Jarcho M. Calcium phosphate ceramics as hard tissue prosthetics. *J Clin Orthop* 1981;157:259–78.
- [39] Breitbart AS, Staffenberg DA, Thorne CH, Glat PM, Cunningham NS, Reddi AH, et al. Tricalcium phosphate and osteogenin: a bioactive onlay bone graft substitute. *J Plast Reconstr Surg* 1995;96(3):699–708.
- [40] Grynblas MD, Pilliar RM, Kandel RA, Renlund R, Filiaggi M, Dumitriu M. Porous calcium polyphosphate scaffolds for bone substitute applications in vivo studies. *Biomaterials* 2002;23(9):2063–70.
- [41] Shimazaki K, Mooney V. Comparative study of porous hydroxyapatite and tricalcium phosphate as bone substitute. *J Orthop Res* 1985;3(3):301–10.
- [42] Steffen T, Stoll T, Arvinte T, Schenck RK. Porous tricalcium phosphate and transforming growth factor used for anterior spine surgery. *Eur Spine J* 2001;10:132–40.
- [43] Hollinger JO, Brekke J, Gruskin E, Lee D. Role of bone substitutes. *J Clin Orthop* 1996;324:55–65.
- [44] Barnes WD, Colowick SP. Stimulation of sugar uptake and thymidine incorporation in mouse 3T3 cells by calcium phosphate and other extracellular particles. *Proc Natl Acad Sci USA* 1977;74(12):5593–7.
- [45] Stiles CD, Capone GT, Scher CD, Antoniades HN, van Wyk JJ, Pledger WJ. Dual control of cell growth by somatomedins and platelet-derived growth factor. *Proc Natl Acad Sci USA* 1979;76(3):1279–83.